

## CONSTRAINTS ON THE EXPLOSION MECHANISM AND PROGENITORS OF TYPE IA SUPERNOVAE

S. Blondin<sup>1</sup>, Luc Dessart<sup>2</sup>, D. John Hillier<sup>3</sup> and Alexei M. Khokhlov<sup>4</sup>

**Abstract.** We present 1D non-LTE time-dependent radiative-transfer simulations of Type Ia supernova (SN Ia) ejecta resulting from different explosion mechanisms and white dwarf (WD) progenitor masses, and confront our results to SN Ia observations over the first  $\sim 100$  d of their evolution. While the “standard” Chandrasekhar-mass delayed-detonation model reproduces the observed properties of SNe Ia near maximum light over a wide range of peak luminosities, the high luminosity and blue optical colours seen at early times in several SNe Ia appears to require some hydrodynamical interaction affecting the outermost ejecta layers, here in the form of a strong pulsation. Moreover, the fast light-curve evolution of the least luminous SNe Ia seem to require WD progenitors below the Chandrasekhar mass. The observed diversity of the SN Ia population can thus be reproduced with multiple progenitor channels and explosion mechanisms. In this context, departures from spherical symmetry only play a minor role.

Keywords: radiative transfer, supernovae

### 1 Introduction

Type Ia supernovae (SNe Ia) likely result from the thermonuclear explosion of a C/O white dwarf (WD) star (Hoyle & Fowler 1960). The energy released from fusion of C/O to iron-peak elements unbinds the star, accelerates the ejecta to velocities  $\sim 10000$  km s<sup>-1</sup>, and synthesizes copious amounts ( $\lesssim 1 M_{\odot}$ ) of <sup>56</sup>Ni to power the light curve ( $L_{\text{bol}} \approx 10^{43}$  erg s<sup>-1</sup> at peak; Colgate & McKee 1969). The “standard” model for SNe Ia consists of a WD approaching the Chandrasekhar-mass limit ( $M_{\text{Ch}} \approx 1.4 M_{\odot}$ ) through accretion of H/He-rich material from a non-degenerate binary companion (Whelan & Iben 1973). Alternatively, such explosions could result from the merger (or collision) of two WDs, in which case the total mass would differ significantly from  $M_{\text{Ch}}$  (Iben & Tutukov 1984; Webbink 1984; see also van Kerkwijk et al. 2010; Pakmor et al. 2012).

In what follows, we present the results from radiative-transfer simulations for three classes of SN Ia models. The explosion hydrodynamics is described by the reactive flow Euler equations of fluid dynamics which are solved with a one-dimensional Lagrangian hydrodynamics code (see Khokhlov 1991). The calculation is carried out until the ejecta mass shells reach a ballistic regime (homologous expansion), less than  $\sim 1$  min past explosion. Detailed nucleosynthesis is calculated by post processing temperature, density, and neutronization histories of fluid elements with a detailed reaction network.

The long-term evolution is computed with the 1D, time-dependent, non-LTE radiative-transfer code CMFGEN (Hillier & Dessart 2012; Dessart et al. 2014c), which includes the treatment of non-local energy deposition and non-thermal effects (e.g., Dessart et al. 2014b). The output of such calculations are light curves and spectra that can be directly confronted to SN Ia observations.

<sup>1</sup> Aix Marseille Universit , CNRS, LAM (Laboratoire d’Astrophysique de Marseille), UMR 7326, 13388 Marseille, France.

<sup>2</sup> Laboratoire Lagrange, UMR 7293, Universit  Nice Sophia-Antipolis, CNRS, Observatoire de la C te d’Azur, 06300 Nice, France.

<sup>3</sup> Department of Physics and Astronomy & Pittsburgh Particle Physics, Astrophysics, and Cosmology Center (PITT PACC), University of Pittsburgh, Pittsburgh, PA 15260, USA.

<sup>4</sup> Department of Astronomy & Astrophysics, the Enrico Fermi Institute, and the Computation Institute, The University of Chicago, Chicago, IL 60637, USA.

## 2 Standard Chandrasekhar-mass models

In this first class of Chandrasekhar-mass models, the burning starts as a subsonic deflagration, followed by a supersonic detonation once the density ahead of the flame front reaches some transition density,  $\rho_{\text{tr}}$ . By varying  $\rho_{\text{tr}}$ , one changes the density at which the detonation wave burns the remainder of the WD, hence the production of  $^{56}\text{Ni}$  at the expense of intermediate-mass elements, and in turn the peak SN Ia luminosity. In Blondin et al. (2013) we explored a grid of such “delayed-detonation” models with  $^{56}\text{Ni}$  masses ranging between  $0.12 M_{\odot}$  and  $0.85 M_{\odot}$ , and found an excellent agreement with SN Ia observations near maximum light, from the luminous SN 2009ig to the low-luminosity SN 1999by (Fig. 1, left).

Moreover, an in-depth study of model DDC15 ( $M_{^{56}\text{Ni}} = 0.51 M_{\odot}$ ) showed that such standard delayed detonations were particularly well suited to SNe Ia with broad Si II 6355 Å lines, such as SN 2002bo (Fig. 1, right; Blondin et al. 2015). The agreement over the first  $\sim 100$  d since explosion suggests the chemical stratification of this model is adequate. Moreover, our assumption of spherical symmetry is not detrimental to reproducing the radiative properties of standard SNe Ia. Interestingly, similar conclusions (chemical stratification and spherical symmetry) are reached from X-ray observations of SN Ia remnants (e.g., Badenes et al. 2006).

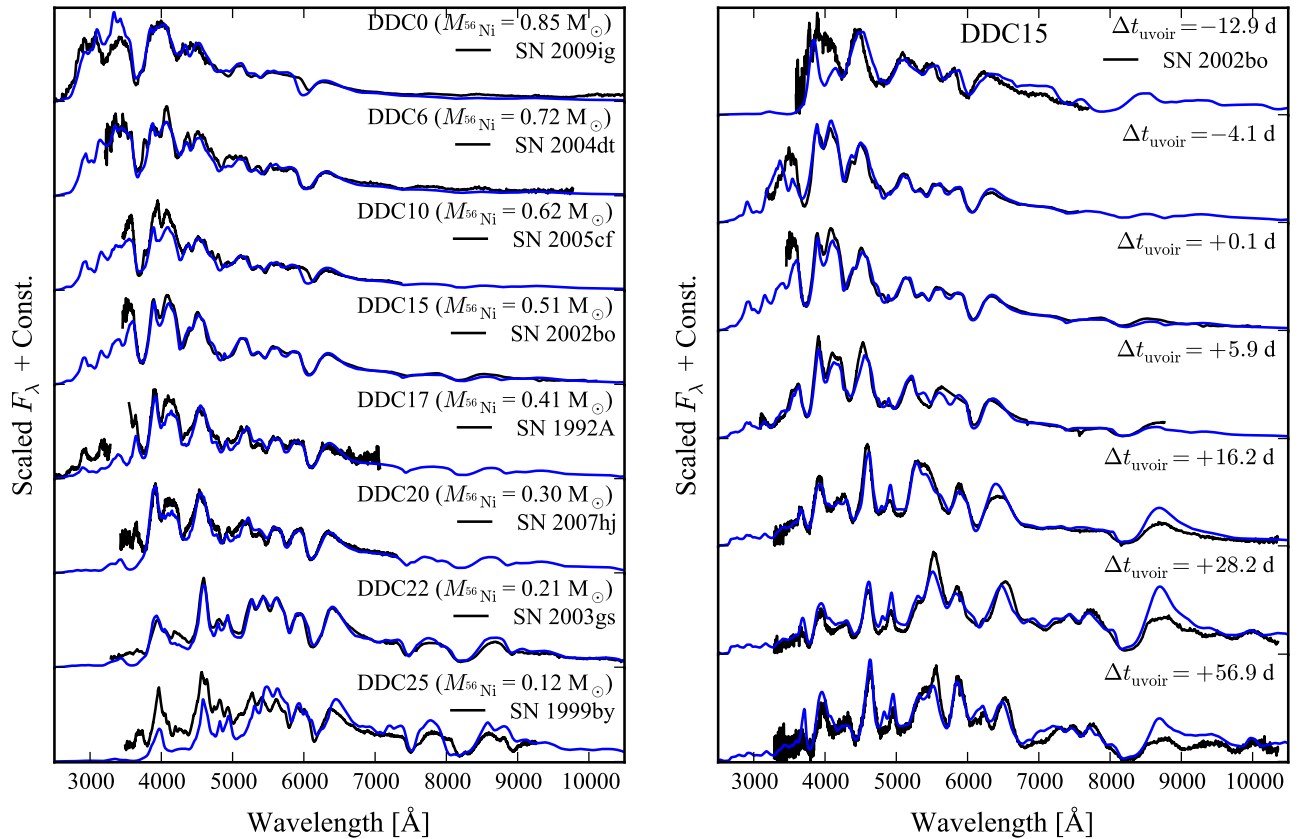


**Fig. 1. Left:** Comparison of synthetic spectra of standard Chandrasekhar-mass delayed-detonation models (blue) to observed SNe Ia near maximum light (black). The models have been ordered by decreasing  $^{56}\text{Ni}$  mass (i.e., decreasing peak luminosity). This figure is similar to Fig. 5 of Blondin et al. (2013) but with updated versions of the models. **Right:** Optical spectroscopic evolution of model DDC15 (blue) compared to SN 2002bo (black), between  $-12.9$  d and  $+56.9$  d from ultraviolet-optical-infrared (“uvoir”) bolometric maximum. See Blondin et al. (2015) for details.

## 3 Pulsating Chandrasekhar-mass models

Despite the successes of the standard delayed-detonation model, the predicted luminosity during the first few days past explosion is too low compared to observations (e.g., the nearby SN 2011fe in M101), and the optical colours too red. Moreover, these models are unable to reproduce the narrow Si II 6355 Å line and the slow

evolution of its velocity at maximum absorption seen in so-called “low-velocity-gradient” (or LVG) SNe Ia, nor the absorption features associated with C II 6580 Å that probe the initial WD composition.

All these problems are overcome with the class of models known as pulsating delayed-detonations (PDD). In our setup, the deflagration is artificially quenched, allowing the inner WD layers to recollapse before the detonation is initiated — the outermost layers escape burning altogether. The hydrodynamical interaction between the (outgoing) detonation wave and the infalling WD material produces a dense shell with a steep density fall-off on its outer edge (the “cliff” at  $\sim 15000 \text{ km s}^{-1}$  in model PDDEL4; see Fig. 2, upper left panel) and a larger temperature in the outer low-density shocked material compared to a standard delayed-detonation model with a similar  $^{56}\text{Ni}$  mass (DDC15; Fig. 2, lower left panel). The result is a higher luminosity at early times, more compatible with that observed for SN 2011fe (Fig. 2, upper right panel), as well as bluer optical colours reflected in the SED at two weeks before maximum light (Fig. 2, lower right panel).

Moreover, the presence of unburnt carbon at lower velocities combined with the higher temperature favours the emergence of C II 6580 Å absorption features seen in some early-time SN Ia spectra. Last, the presence of a density “cliff” results in a slower evolution of the spectrum-forming region in velocity space, and hence offers a natural explanation for SNe Ia of the LVG subclass. Interestingly, the association of C II detections with LVG events has been confirmed observationally by several authors (e.g., Parrent et al. 2011).

Such a “pulsation” configuration affects the outer ejecta layers and hence can bring diversity at early times in a spherically-symmetric ejecta and independent of the  $^{56}\text{Ni}$  mass, which affects the evolution around maximum light and beyond. Despite the artificial setup, these models illustrate the impact of a hydrodynamical interaction on the predicted observables, as could arise for instance in a binary WD merger event.

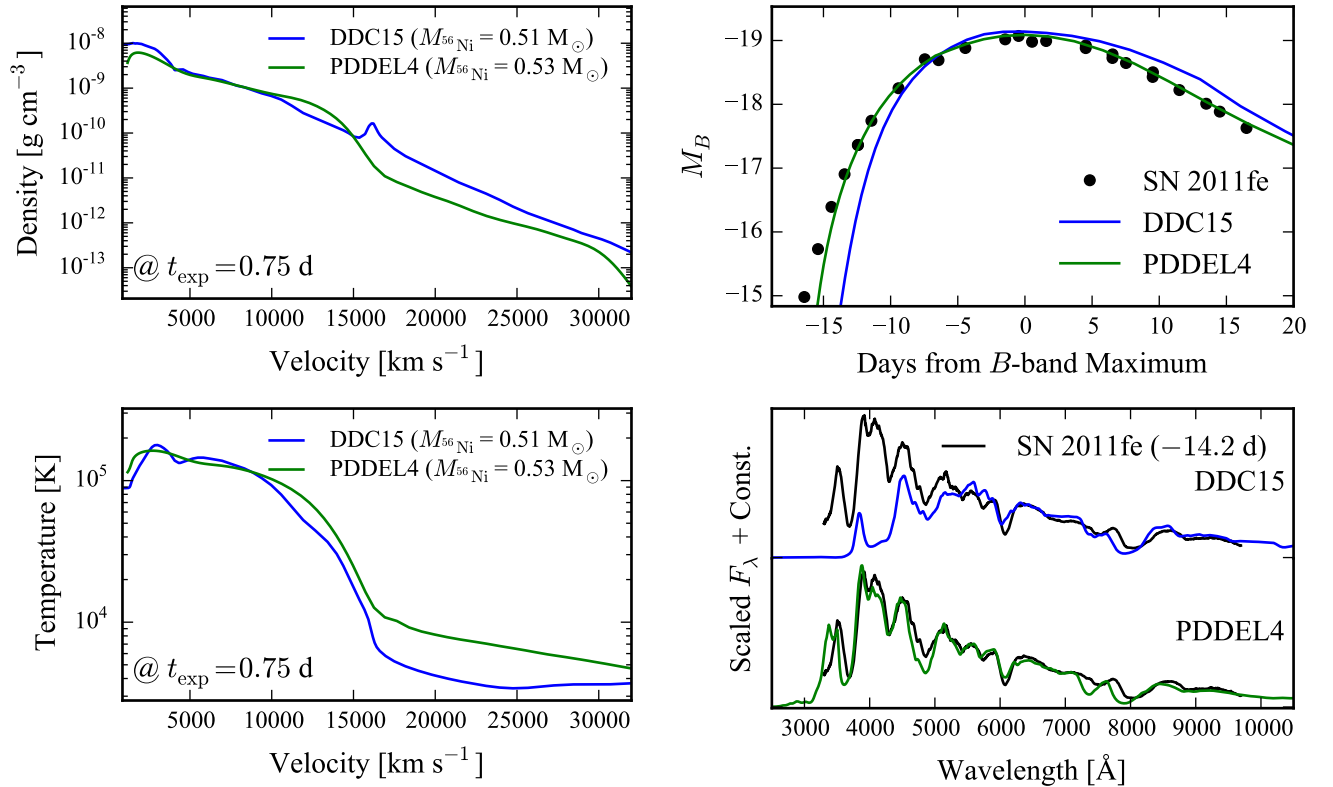


**Fig. 2. Left:** Density (upper panel) and temperature (lower panel) profiles at 0.75 d past explosion for the standard Chandrasekhar-mass delayed-detonation model DDC15 (blue) and the pulsating Chandrasekhar-mass delayed-detonation model PDDEL4 (green). Note the density “cliff” at  $\sim 15000 \text{ km s}^{-1}$  and the hotter outer ejecta layers in the pulsating model. **Right:** Comparison of the absolute  $B$ -band light curves (upper panel) and spectra at  $-14 \text{ d}$  from maximum light (lower panel) of models DDC15 and PDDEL4 to corresponding observations of SN 2011fe. The model spectra have been scaled to match the  $V$ -band flux of SN 2011fe. The hotter outer ejecta in the pulsating model result in a more luminous and bluer event at early times. See Dessart et al. (2014a) for details.

#### 4 Sub-Chandrasekhar-mass models

With the two classes of Chandrasekhar-mass delayed-detonation models discussed above it appears one can reproduce the full range of observed SN Ia luminosities while accounting for some diversity at a given peak luminosity. However, these models fail to reproduce the fast light-curve evolution for the least luminous events, similar to the prototypical SN 1991bg (cf. the  $V$ -band light curve for model DDC25 compared to the “91bg-like” SN 1999by in the right panel of Fig. 3). The main reason lies in the amount of mass above the (centrally concentrated)  $^{56}\text{Ni}$ -rich layers: for our Chandrasekhar-mass model DDC25, 99% of the total  $^{56}\text{Ni}$  mass ( $\sim 0.12 M_{\odot}$ ) is located at a mass coordinate  $\lesssim 0.8 M_{\odot}$ , i.e.  $\sim 0.6 M_{\odot}$  below the WD surface layers (Fig. 3, left).

The explosion of WDs below the Chandrasekhar mass offers an attractive alternative to the delayed-detonation models. For these low-mass WDs, the ignition of the C/O fuel can result either indirectly through the surface detonation of a thin He-rich accreted layer leading to compression of the core (“double-detonation”), or through a WD-WD merger whose combined mass is less than  $\sim 1.4 M_{\odot}$ .

In our sub-Chandrasekhar-mass model SCH2p0, corresponding here to the pure detonation of a  $0.88 M_{\odot}$  C/O WD star, the same amount of  $^{56}\text{Ni}$  extends over a larger fraction of the total ejecta mass, leading to a shorter diffusion time for radiation, and hence a faster rise to peak ( $\sim 16$  d cf.  $\sim 21$  d to bolometric maximum). The post-maximum luminosity decline is also faster, since the lower ejecta densities favour the direct escape of  $\gamma$ -rays and leakage of optical photons. Sub-Chandrasekhar-mass models thus lead to narrower light curves for a given  $^{56}\text{Ni}$  mass (and hence peak luminosity), in better agreement with the observed width-luminosity relation of Phillips (1993) for the least luminous events.

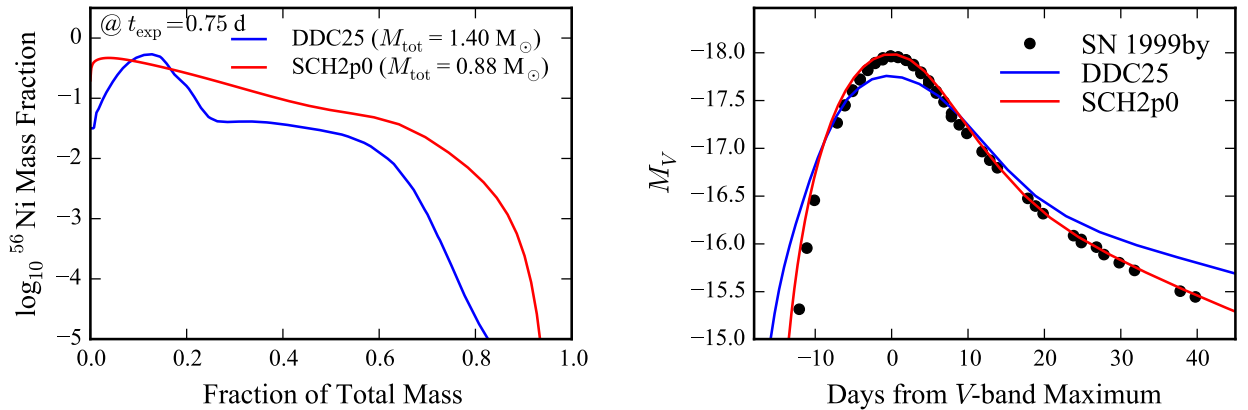


**Fig. 3. Left:** Abundance profile for  $^{56}\text{Ni}$  vs. the fractional mass coordinate ( $\equiv M_{\text{Lagrangian}}/M_{\text{tot}}$ ) for the standard Chandrasekhar-mass delayed-detonation model DDC25 (blue) and the sub-Chandrasekhar-mass model SCH2p0. **Right:** Absolute  $V$ -band light curves of both models compared to the low-luminosity (“91bg-like”) SN 1999by, for which we assume a distance modulus of 30.97 mag and a host-galaxy visual extinction  $A_V = 0.11$  mag. The lower ejecta mass for model SCH2p0 results in a faster light-curve evolution around maximum light.

#### 5 Conclusions

We have presented three classes of SN Ia models resulting from different explosion mechanisms and white dwarf (WD) progenitor masses. Neither model on its own is able to reproduce the full range of SN Ia properties, suggesting the observed diversity results from multiple progenitor scenarios and explosion mechanisms. Differentiating between these different scenarios requires detailed radiative-transfer calculations, currently only feasible in 1D. While the explosion is expected to be an intrinsically multi-dimensional process, the resulting SN Ia ejecta appear well reproduced by spherically-symmetric models. We will nonetheless compare our 1D models to angle-averaged versions of multi-D calculations in the future.

All our model results are available online at: <https://www-n.oca.eu/supernova/home.html>.

from the “Programme National de Physique Stellaire” (PNPS). DJH acknowledges support from STScI theory grant HST-AR-12640.01, and NASA theory grant NNX14AB41G. This work was granted access to the HPC resources of CINES under the allocation c2013046608 and c2014046608 made by GENCI (Grand Equipement National de Calcul Intensif).

## References

- Badenes, C., Borkowski, K. J., Hughes, J. P., Hwang, U., & Bravo, E. 2006, *ApJ*, 645, 1373
- Blondin, S., Dessart, L., & Hillier, D. J. 2015, *MNRAS*, 448, 2766
- Blondin, S., Dessart, L., Hillier, D. J., & Khokhlov, A. M. 2013, *MNRAS*, 429, 2127
- Colgate, S. A. & McKee, C. 1969, *ApJ*, 157, 623
- Dessart, L., Blondin, S., Hillier, D. J., & Khokhlov, A. 2014a, *MNRAS*, 441, 532
- Dessart, L., Hillier, D. J., Blondin, S., & Khokhlov, A. 2014b, *MNRAS*, 439, 3114
- Dessart, L., Hillier, D. J., Blondin, S., & Khokhlov, A. 2014c, *MNRAS*, 441, 3249
- Hillier, D. J. & Dessart, L. 2012, *MNRAS*, 424, 252
- Hoyle, F. & Fowler, W. A. 1960, *ApJ*, 132, 565
- Iben, Jr., I. & Tutukov, A. V. 1984, *ApJS*, 54, 335
- Khokhlov, A. M. 1991, *A&A*, 245, 114
- Pakmor, R., Kromer, M., Taubenberger, S., et al. 2012, *ApJ*, 747, L10
- Parrent, J. T., Thomas, R. C., Fesen, R. A., et al. 2011, *ApJ*, 732, 30
- Phillips, M. M. 1993, *ApJ*, 413, L105
- van Kerkwijk, M. H., Chang, P., & Justham, S. 2010, *ApJ*, 722, L157
- Webbink, R. F. 1984, *ApJ*, 277, 355
- Whelan, J. & Iben, I. J. 1973, *ApJ*, 186, 1007